5 Biomembranes

5.1 Motivation

Biological membranes are thin, flexible, selectively permeable surfaces that separate cells and their organelles from their environments. Biomembranes form closed structures with an internal face oriented toward the interior of the compartment and an external face presented to the environment. Each type of cellular membrane has certain distinctive activities determined largely by the unique set of proteins associated with that membrane. We can distinguish two different types of membrane proteins (i) integral proteins, which partly or entirely penetrate the membrane, and (ii) peripheral proteins, which are laterally attached to one side of the membrane. Biomembranes are

Figure 5.1: Electron microscopy of the cell membrane stained with osmium tetroxide illustrating the polar head groups with a light 2nm space of hydrophobic tails sandwiched between them, adopted from [5]

typically asymmetric, their interior and exterior faces can carry different proteins and have different properties. Although biological membranes may have different properties and functions, all membranes share a common structural architecture that we will address in this chapter. They are rich in phospholipids, which spontaneously form a characteristic bilayer structures in water. Membrane proteins and lipids can diffuse laterally or sideways throughout the membrane, giving them their characteristic appearance of a fluid rather than a solid.
Given the variable composition of cellular membranes, how can we be that the phospholipid bilayer structure is common to all biomembranes? Electron microscopy of thin membrane sections provides the most direct evidence for the universality of the bilayer structure. Osmium tetroxide can be used for staining of phospholipids since it binds strongly to the polar head groups. A cross section of a single membrane stained with osmium tetroxide looks like a railroad track. Figure 5.1 shows two thin dark lines, the stained head group complexes, and a uniform 2nm light space of the hydrophobic tails sandwiched between them.

5.1.1 Micropipette aspiration

Micropipette aspiration is one of the oldest techniques to measure the mechanical properties of cells [2, 12, 18, 26, 43]. It produces a deformation pattern opposite to that generated by atomic force microscopy and optical traps or laser tweezers in that the cell surface is stretched into a small pipette rather than compressed into the cell interior. By

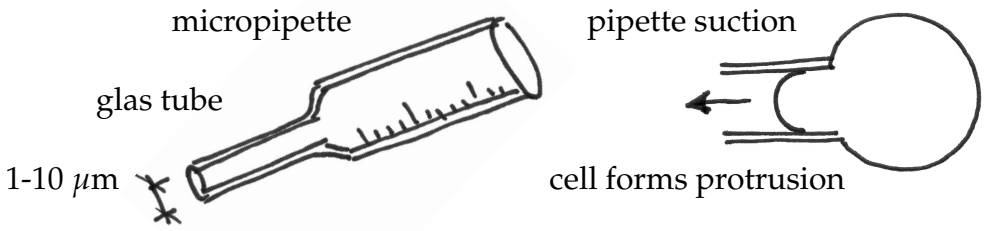

Figure 5.2: During micropipette aspiration, a cell is aspired into a thin glass tube. Knowing the applied suction pressure, we can determine the surface tension of the cell based on changes in cell geometry.

exploring how cells respond to the applied pressure, we hope to understand how cells can flow through small vessels, how molecular structure influences their mechanical behavior and how mechanical and chemical stimuli might alter their response. During micropipette aspiration, the surface of a cell is aspirated into a small glass tube while tracking the leading edge in a light microscope, see Figure 5.2. A typical pipette diameter is 1-10 μm and surface edges can be tracked to an accuracy of ± 23 nm. Figure 5.3

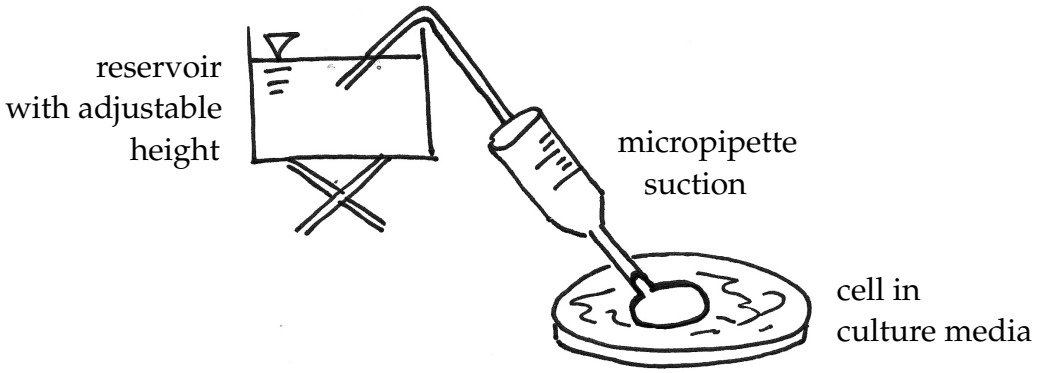

Figure 5.3: Experimental setup of micropipette aspiration. The applied suction pressure can be varied by adjusting the height of a fluid filled reservoir. Cell deformation is measured optically.

shows a common experimental setup of micropipette aspiration. A cell suspended in a saline solution is partially aspirated into the mouth of the pipette. Suction pressures as small as 0.1-0.2 pN/μm^2 can be applied by adjusting the height of a fluid reservoir attached to the pipette. Knowing the applied pressure, we can determine the surface tension of the cell based on changes in protrusion geometry. Micropipette aspiration is suited for both rigid cells such as chondrocytes and endothelial cells with an elastic modulus of 500 pN/μm^2, and for soft cells such as neutrophils and red blood cells with a surface tension of 30 pN/μm and a viscosity of 100 Pa s.

Micropipette aspiration is a dynamic procedure and we can distinguish three stages during the aspiration process. Figure 5.4 displays the initial state, the critical state, and the final state of the aspiration process. Initially, the protrusion radius R^{pro} is larger than the protrusion length L^{pro} and the sucked in part looks like a pimple as $L^{\text{pro}}/R^{\text{pro}} < 1$, Figure 5.4, left. As the pressure is gradually increased, the cell gets

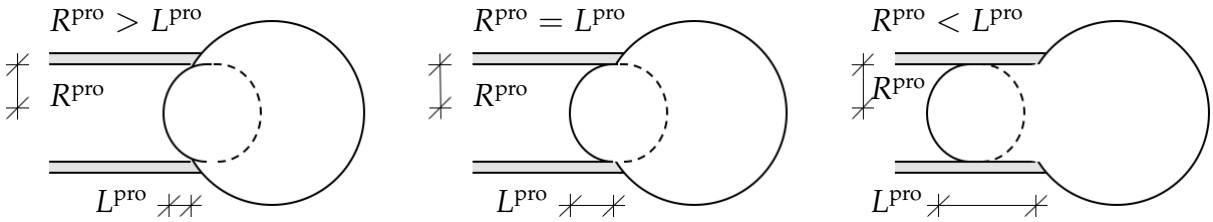

Figure 5.4: The three stages during mircopipette aspiration. The initial state with $L^{\text{pro}}/R^{\text{pro}} < 1$, left, the critical state with $L^{\text{pro}}/R^{\text{pro}} = 1$, middle, and the final state with $L^{\text{pro}}/R^{\text{pro}} > 1$, right.

more and more sucked into the pipette until the protrusion radius is equal to the protrusion length $L^{\text{pro}}/R^{\text{pro}} = 1$, Figure 5.4, middle. Increasing the pressure further generates a hotdog shape state in which $L^{\text{pro}}/R^{\text{pro}} > 1$, Figure 5.4, right. Eventually, the entire might rush into the pipette. Figure 5.5 illustrates the states of micropipette aspiration. As the suction pressure is gradually increased, a larger part of the cell is sucked into the pipette. Early experiments with neutrophils, which have a radius of

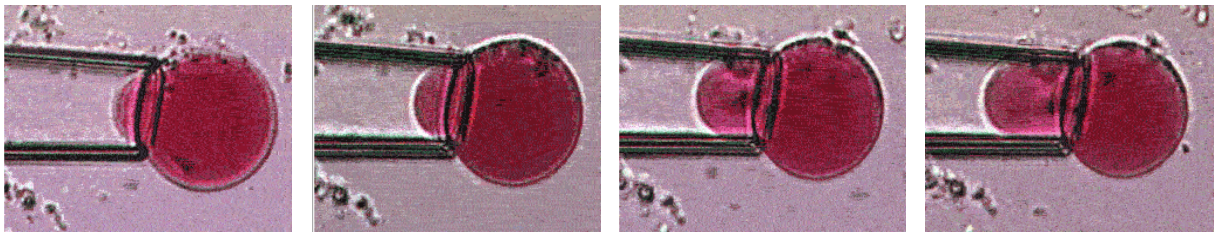

Figure 5.5: Experimental observation of different stages during micropipette aspriation adopted from http://newton.ex.ac.uk/research/biomedical/membranes.

approxiamtely $R^{\text{cell}} \approx 4\,\mu$m revealed a strange behavior [12, 43]. After the critical state of $L^{\text{pro}}/R^{\text{pro}} = 1$, the entire cell flushed into the pipette although the pressure was not increased significantly. Experiments with different micropipette radii of 1.0-3.75 μm and different suction pressures of 10^2-10^4 dyn/cm^2 always yielded similar results [12]. Can the micropipette aspiration experiment help to explain the cellular rheology and microstructure responsible for this behavior?

When studying the literature, we will find two fundamentally different whole cell models: (i) the liquid drop model and (ii) the elastic solid model. In the liquid drop model, the cell is considered as a fluid filled balloon with an elastic cortical membrane whereas in the elastic solid model, the cell is considered as a homogeneous elastically deformable material. Although fundamentally different, both models make good predictions of the mechanical behavior of the cell during micropipette aspiration. This is even more surprising as that the cellular microstructure is extremely heterogeneous

consisting of a complex cytoplasm with granules, various types of filaments, a nucleus, and dissolved proteins. The micropipette aspiration experiment can provide guidelines which if the two models is more appropriate for a given cell type.

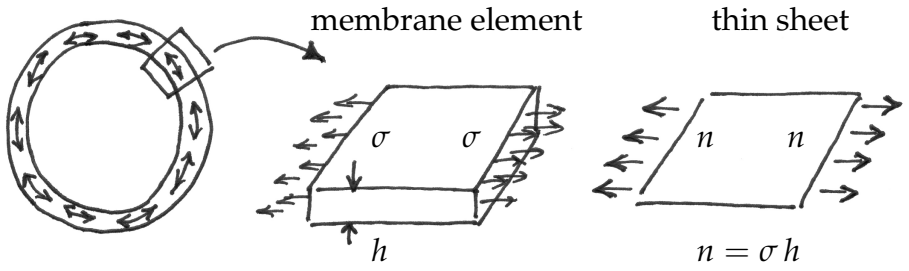

Figure 5.6: Liquid drop model. The internal fluid pressure is balanced by a thin elastic shell. The membrane element of thickness h is subjected to membrane stresses σ. Equivalently, the membrane can be represented as a thin sheet subjected to the surface tension n which results from the integration of the membrane stress over the thickness as $n = \sigma\, h$.

Assuming everybody has a pretty good idea what an elastic solid is, we will focus on the liquid drop model for now. It can be represented mechanically through a thin spherical membrane loaded by an internal fluid pressure. Figure 5.6 illustrates the spherical shell with an infinitesimal membrane element. Membrane stresses σ are assumed to act across the thickness h. It is common to approximate the membrane as a thin sheet. By integrating its membrane stresses across the thickness,

$$n = \sigma\, h \qquad \text{with} \qquad [\,n\,] = [\,\text{force / length}\,] \qquad \ldots \quad \text{surface tension} \tag{5.1.1}$$

we obtain the surface tension $n = \sigma\, h$ as the normal stress resultant, the force per unit length n. But how can we measure the surface tension n?

Law of Laplace

The law of Laplace is more than two hundred years old [25]. It tells us how much a cell would blow up under a certain pressure, or, more precisely, it provides a relation between the radius R of a membrane subjected to the pressure difference $\Delta p = p^{\text{int}} - p^{\text{out}}$, where p^{int} and p^{out} are the pressures inside and outside the cell, respectively. As

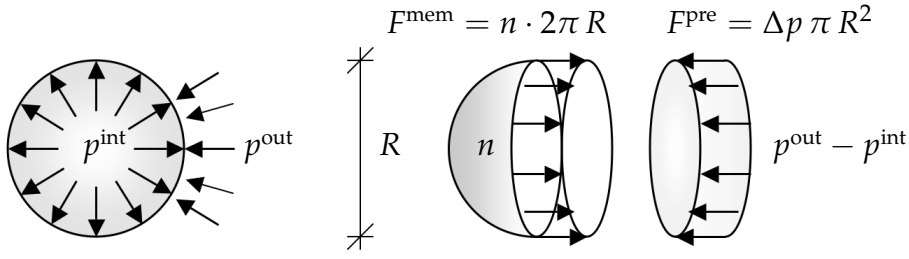

Figure 5.7: Law of Laplace. The membrane force $F^{\text{mem}} = n \cdot 2\pi\, R$ is the result of the surface tension n acting on the cell membrane along the circumference $C = 2\,\pi\, R$. It is in equilibrium with the forces F^{pre} resulting from the pressure difference Δp acting on the cell area $A = \pi\, R^2$.

indicated in figure 5.7, we can then simply draw a free body diagram of a cell cut in half and write down the force balance

$$F^{\text{mem}} \doteq F^{\text{pre}} \tag{5.1.2}$$

where

$$F^{\text{mem}} = n\,C \qquad \text{with} \qquad C = 2\,\pi\,R \tag{5.1.3}$$

are the forces of the cell membrane acting along the circumference C and

$$F^{\text{pre}} = [\,p^{\text{int}} - p^{\text{out}}\,]\,A \qquad \text{with} \qquad A = \pi\,R^2 \tag{5.1.4}$$

are the forces generated by the pressure difference across the cell wall acting on the surface area A. When combining these three equations, we obtain the law of Laplace

$$\Delta p = p^{\text{int}} - p^{\text{out}} = 2\,\frac{n}{R} \qquad \text{... law of Laplace} \tag{5.1.5}$$

giving a relation between the pressure difference of the wall and the curvature of the cell $1/R$ in terms of the surface tension n.

Surface tension

Now, let's return to the micropipette aspiration experiment and let's look at the limit case for which $L^{\text{pro}} = R^{\text{pro}} = R^{\text{pip}}$ as depicted in Figure 5.8.

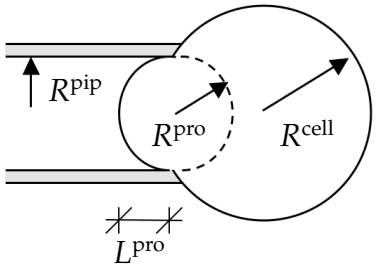

Figure 5.8: Kinematics of micropipette aspiration. For the limit state, at $L^{\text{pro}}/R^{\text{pro}} = 1$, the law of Laplace can be used to determine the surface tension n.

For this limit case, we can state the law of Laplace for the protrosion, with both the pipette pressure and the intracellular pressure acting in the same direction, to the left in Figure 5.8,

$$p^{\text{pip}} + p^{\text{int}} - p^{\text{out}} = 2\,n\,\frac{1}{R^{\text{pip}}} \qquad \text{... law of Laplace for the protrusion} \tag{5.1.6}$$

and we can state the law of Laplace for cell itself.

$$p^{\text{int}} - p^{\text{out}} = 2\,n\,\frac{1}{R^{\text{cell}}} \qquad \text{... law of Laplace for the cell} \tag{5.1.7}$$

Subtracting the two expressions, we obtain the following relation to determine the surface tension n.

$$p^{\text{pip}} = 2\,n \left[\frac{1}{R^{\text{pip}}} - \frac{1}{R^{\text{cell}}} \right] \tag{5.1.8}$$

In a series of experiments with different pressures and micropipettes of different diameter, the surface tension of neutrophils, white blood cells, was found to be n=35 pN/μm [12]. Both red and white blood cells are particularly interesting and have been studied a lot since they undergo large deformations when passing through tiny capillaries. Their membranes are hard to stretch, but easy to shear and bend!
So why do some cell types flow into the pipette beyond the limit point of $L^{\text{pro}}/R^{\text{pro}} = 1$? Let's look at the above equation again. We increase the pressure Δp. The surface tension is a material property, and thus constant for a given cell type. The protrusion radius is limited by the pipette radius $R^{\text{pro}} = R^{\text{pip}}$. So if we increase the pressure Δp, the cell radius will decrease R^{cell}. As soon as it reaches the radius of the pipette $R^{\text{cell}} = R^{\text{pip}}$, the cell will flush into the pipette.

Liquid drop or elastic solid?

So, what can we learn from the micropipette experiment if for large enough pressures, all cell are eventually sucked into the pipette? The experiment can tell us two things: (i) Before the critical limit point $L^{\text{pro}}/R^{\text{pro}} = 1$, we can determine the surface tension n for all cell types. (ii) Beyond the critical limit point $L^{\text{pro}}/R^{\text{pro}} = 1$, we can tell whether the cell behaves more like a liquid drop, i.e., it rushes into the pipette without further resistance, or more like an elastic solid, i.e., the pressure can be further increased as the cell gets sucked in gradually. When cells that behave as solids are aspirated into a micropipette, obviously they do not flow into the pipette when the $L^{\text{pro}}/R^{\text{pro}} > 1$. Chondrocytes, for example, are much stiffer than red and white blood cells. Their aspiration length increases linearly with the suction pressure regardless of the value for L^{pro}. This leads us to believe that chondrocytes behave as elastic solids. It's important to keep in mind that we can only make statements on whether the cell behaves as a liquid drop or as an elastic solid if the pressure is increased beyond the critical point.

Finite element simulation of micropipette aspiration

Similar to all cell experiments that are based on observing cell or cell membrane deformation, the observations can only be interpreted by using mechanical models and making reasonable assumptions. Both the liquid drop model and the elastic solid model are based on continuum theories and assume that the stress distribution in the cell is homogeneous. Finite element simulations can take into account large deformations, inhomogeneous stress profiles, and a more realistic representation of the boundary conditions at the micropipette interface. Figure 5.9 shows a micropipette aspiration experiment with chondrocytes which behave as an elastic solid. Figure 5.10 depicts the

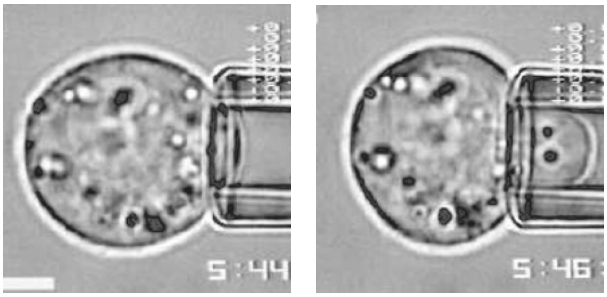

Figure 5.9: Micropipette aspiration of chondrocytes behaving as elastic solids with a protrusion length L^{pro} increasing linearly with the applied suction pressure Δp even beyond the critical limit point of $L^{\text{pro}}/R^{\text{pro}} = 1$, adopted from [2].

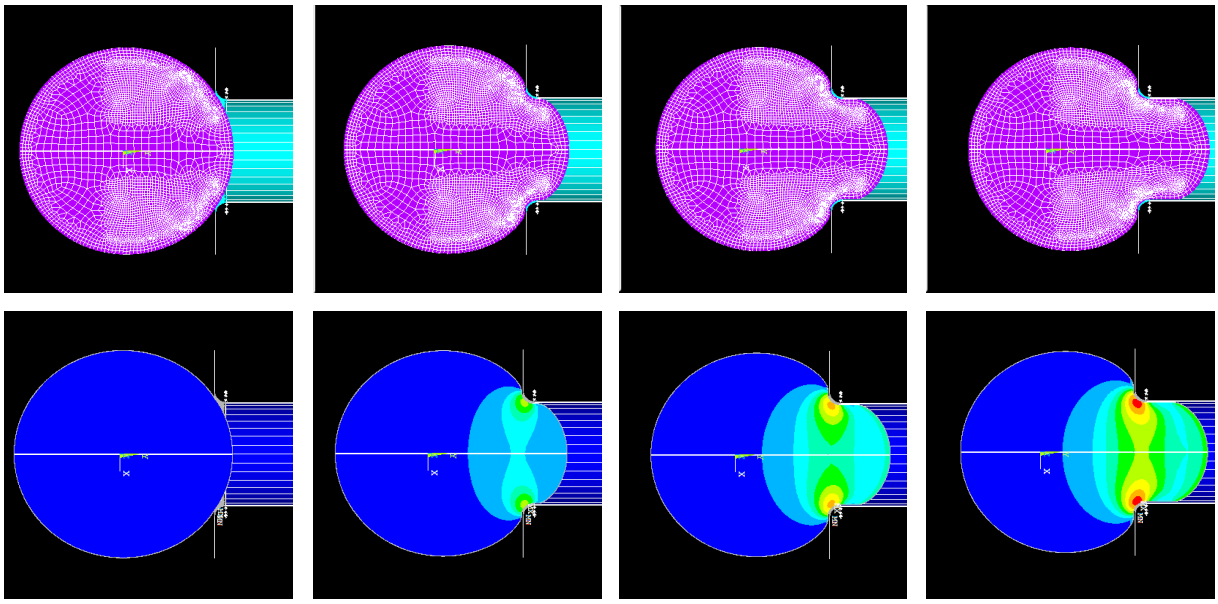

Figure 5.10: Finite element simulation of micropipette aspiration of a chondrocyte modeled as an elastic solid. In contrast to analytical results, finite element simulations can account for large deformations, heterogeneous stress distributions, and a more realistic representation of the boundary conditions [21].

corresponding finite element simulation. For the computational simulation, Young's modulus is chosen as $E = 2.55$kPa and Poisson's ratio is $\nu = 0.4$. The applied suction pressure varies between $\Delta p = 255$ Pa and $\Delta p = 765$ Pa. Frictionless contact is assumed between the cell and the glass pipette which is assumed to be of soda-lime with a Young's modulus of $E = 9{\cdot}10$ Pa and Poisson's ratio of $\nu = 0.22$. Contact is solved by means of an augmented Lagrange method, a penalty method with penetration control. During the deformation the free cellular surface keeps the same curvature and the contact surface of the cell deforms along the micropipette sidewall, see Figure 5.10. In the stress plot shown in the bottom row the largest stress occurs at the point close to the transition between the fillet and the inner wall of the pipette. This stress reaches 1500 Pa when the applied pressure is 765 Pa. This result is in good agreement with patch clamp experiments.